Laser Velocimeter for Studies of Microgravity Combustion Flowfields
Grant NAG3-2240

Philip L. Varghese
The University of Texas at Austin
Department of Aerospace Engineering and Engineering Mechanics

ABSTRACT

A velocimeter was developed based on modulated filtered Rayleigh scattering (MFRS). The MFRS velocimeter was successfully demonstrated by making one-component velocity measurements in a supersonic expansion using molecular Rayleigh scattering in a jet of N_2. These measurements were made in a sweep mode where the Rayleigh scattered profile is cross-correlated with absorption in a static cell to determine velocity. To improve temporal resolution the frequency-locked mode of operation was developed, with an in-situ referencing scheme to compensate for signal fluctuations arising from density variations in the probe volume. Spectroscopic grade (i.e. continuously tunable, single-mode) laser sources with high power (>100 mW) are not commercially available at the wavelength of interest (780 nm). We developed an all-solid-state system with a low power (~10 mW) spectroscopic grade laser source in a Littrow cavity is amplified by a broad-area diode laser. We have demonstrated that the slaved output tracks the injected input but have not yet demonstrated power gain by the end of the grant period.

1. INTRODUCTION

Modulated filtered Rayleigh scattering (MFRS) is a novel variation of filtered Rayleigh scattering (FRS), where standard techniques for detection of weak absorptions by modulation spectroscopy are adapted to detect the strong absorption of the weak Rayleigh scattered signal that is generated with commercially available diode lasers.[1]

The MFRS velocimeter described in this report utilizes a rubidium vapor filter to provide the relatively strong absorption. Alkali metal vapors have a high optical depth at modest vapor pressures, and their narrow linewidth is ideally suited for high-resolution velocimetry. Rubidium has strong absorption lines at 794 nm (D_1) and 780 nm (D_2), respectively. When this work began a GaAlAs single-mode diode laser rated at 50 mW at 780 nm was used to generate the relatively weak Rayleigh scattered signal in the experiment.

Diode lasers offer an inexpensive alternative to other tunable laser systems. In addition, the compact, rugged construction of diode lasers makes them ideally suited for applications in industry, space, and other hostile environments. The modest *cw* power output of diode lasers is compensated for by their rapid and continuous tuning capability which enables heterodyne detection of the weak modulated Rayleigh signal.

Near infrared diode lasers emitting close to 100 mW of continuous single-mode power were commercially available when we began this work in 1999. The telecommunication industry is the chief driver of diode laser technology at this near-infrared wavelength. Since the inception of this work in 1999 the availability of high power single mode lasers at 780 nm has actually decreased because of the industry shift to 1.3 μm technology. Higher power diode laser systems utilizing diode arrays, broad stripe diodes, or tapered semiconductor lasers at 780 nm have also been developed, but have to be modified to provide the narrow linewidth required for accurate velocity measurements using MFRS. Hence, after successful demonstration of proof of concept we had to shift our efforts to developing a spectroscopic grade source of sufficient power to enable velocity measurements in the low density, low velocity gases that are expected in microgravity flame studies.

2. THEORY

Velocity measurements with lasers avoid the drawbacks associated with the introduction of a physical probe into the flow being interrogated. Molecular Rayleigh scattering of laser light simplifies the measurement as it obviates the complications of flow-seeding. Filtered Rayleigh scattering is an established technique for measuring flow velocity and thermodynamic properties in a gas or a flame.[2-9] When laser light at a particular centerline wavelength λ_o is scattered from a target with velocity V, it is Doppler shifted in frequency according to

$$\Delta\nu_{Doppler} = \frac{V}{\lambda_o}\left[\mathbf{i}_v \bullet \left(\mathbf{i}_S - \mathbf{i}_L\right)\right]. \tag{1}$$

The unit vectors in brackets define the geometry of the experiment: $\mathbf{i}_v$, $\mathbf{i}_S$, $\mathbf{i}_L$ are the unit vectors in the direction of the gas velocity, the scattered light, and the laser beam propagation respectively. The MFRS velocity measurements in unseeded flows described in this paper are restricted to a single-component of velocity. However, Eq. 1 shows that it is possible to measure two orthogonal velocity components simultaneously at a point in the flow using a single laser beam by collecting scattered light in opposite directions and we have demonstrated this in our laboratory.[10]

Modulation techniques are utilized to improve detectability of the weak Rayleigh scattered signal. In the current experiment the laser power in the probe volume after spatial filtering is approximately 24.5 mW. The feasibility and technical challenges arising when using relatively low power diode lasers for filtered Rayleigh scattering experiments are illustrated in the following sample calculation.

The Rayleigh scattered signal power P_R is given by[11]

$$P_R = n\left(\frac{\partial\sigma}{\partial\Omega}\right)\Omega_c \cdot \ell \cdot P_{PV}, \tag{2}$$

where n is the number density in the probe volume, $\left(\frac{\partial\sigma}{\partial\Omega}\right)$ is the differential cross-section for Rayleigh scattering (1.30×10^{-28} cm^2/sr at 780 nm)[12], Ω_c is the collection solid angle, ℓ is the length of the probe volume as viewed by the collection optics, and P_{PV} is the laser power at the probe volume. Consider the isentropic expansion of N_2 to 1 atm through a converging nozzle from stagnation conditions of 298 K and 2.1 atm. The number density in the sonic jet core is n =

3.3×10^{19} molecules/cm^3, and for F/1.2 collection optics (Ω_c=0.483 sr) and ℓ = 1 mm, the Rayleigh scattered signal power is approximately 5 pW.

If we assume a transmission efficiency of 65% through the collection optics, rubidium absorption cell, and narrowband filters, and a photomultiplier tube (PMT) with radiant sensitivity of 2.8×10^4 A/W then the filtered Rayleigh signal gives a photocurrent of 92 nA or a voltage of 4.6 μV across an impedance of 50 Ω. These signal levels are detectable provided interference from ambient light fluctuations are minimized. This is achieved with narrow band optical filters centered at 780 nm and with heterodyne detection using lock-in amplifiers.

In order to implement heterodyne detection we utilize the tunability of diode lasers. The ouput frequency of a diode laser varies with injection current, because of changes in the carrier density in the active layer and changes in temperature resulting from Joule heating. However, temperature change is the dominant effect for time scales greater than approximately 1μs, i.e. changing the injection current is essentially a means of rapidly changing the cavity temperature.[13] The diode laser frequency tunes with temperature because of the change in the optical path length of the cavity between the facets and a change in the index of refraction of the active layer, both resulting in a shift in the lasing mode wavelength.

The injection current, and hence the frequency, of the diode laser is dithered at the rate of several kHz while simultaneously sweeping the output frequency across the Rb resonance using a current ramp. The Doppler shifted Rayleigh scattered light is also swept across the resonance. The high frequency modulation results in a modulated absorption through the rubidium filter and a corresponding modulation appears in the PMT output that is fed into the lock-in amplifier. If the lock-in amplifier is synchronized with the function generator that drives the frequency modulation, then very high levels of background rejection are possible because the lock-in is both frequency and phase selective.[14]

In sweep mode MFRS experiments the lock-in amplifier is set at the 2nd-harmonic of the modulation frequency (*2f* detection). A lock-in tuned to the nth-harmonic of the modulation frequency approximates the nth-derivative of the detected signal. Figure 1 shows the conventional absorption profile of the D_2 line of Rb and the corresponding lock-in output for *2f* detection of the detector signal when the laser frequency is dithered during the sweep.

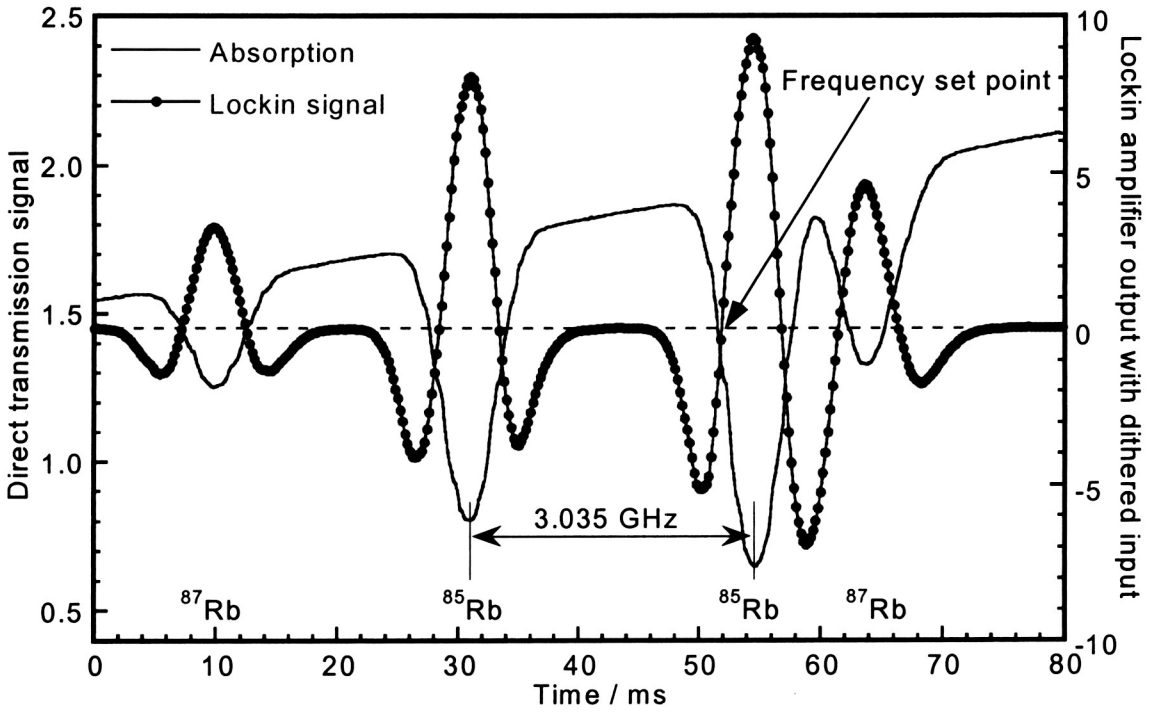

Fig. 1 Hyperfine structure of the D_2 line of Rb in a static cell observed in direct absorption and via modulation spectroscopy with *2f* detection.

The resemblance of the lock-in signal at *nf* to the n^{th}-derivative of the absorption profile depends on the modulation depth and the response rate of the detection electronics relative to the sweep rate. The latter is generally set by the lock-in amplifier output time constant which needs to be increased to improve signal-to-noise ratios (S/N). However, the velocity data rate increases with reduced sweep time so a compromise must be adopted. The signal level increases with modulation depth; although large modulation amplitude results in a somewhat distorted derivative profile, the shape is well understood.[15] Distortions of the observed profile also occur if the sweep time across the profile is comparable to the lock-in amplifier output time constant. The data shown in Fig. 1 correspond to direct absorption measurements in a reference cell. These data correspond to high signal levels, and thus the lock-in time constant could be very small and still obtain high S/N with a relatively rapid sweep of O(100 ms). For Rayleigh scattering measurements the S/N is poorer and so the lock-in output time constant has to be longer for good S/N, and the sweep period is correspondingly increased and the velocity data rate reduced.

3. EXPERIMENTAL SETUP FOR SWEEP MODE OF OPERATION

The experimental setup that was used to make velocity measurements in the "sweep mode" is shown in Figure 2. The single-mode GaAlAs diode (Hitachi HL7851), mounted in a diode laser head (ILX Lightwave LDM-4420), is excited with an ultra-low noise current controller (ILX Lightwave LDX-3620) that is specified to be stable to ≤10 ppm over 10-30 minutes. The temperature of the diode was controlled with a spectroscopic grade thermoelectric temperature controller (ILX Lightwave LDT-5910B) with a long-term stability of less than ±0.01°C. Dry nitrogen is bled into the laser head to prevent condensation during operation. The diode emits at 780 nm when operating at approximately 125 mA and -3°C with a linear tuning rate of approximately -2.1 GHz/mA. Therefore, a triangular current ramp of amplitude 5 mA scans repetitively across the entire hyperfine structure of the D_2 line which extends over approximately 10.5 GHz at Doppler limited resolution. The optimal modulation depth is theoretically about 2.2 times the half width at half maximum (HWHM) of the feature being resolved.[16] At room temperature the Doppler-broadened linewidth of Rb is approximately 250 MHz (HWHM) so a modulation current amplitude of 0.27 mA should result in optimal profile resolution though the modulation depth is generally set slightly higher to improve signal strength. The modulation sine wave and triangular sweep are produced by separate function generators (Exact 200MSP and Stanford Research Systems DS345) and combined in a summing amplifier (Stanford Research Systems SR560) before input to the current driver.

The laser beam is collimated and a small portion (< 1%) of the beam is split off to a reference arm, and passes through a 10 cm long room temperature cell containing Rb vapor in natural isotopic abundance (72.2% ^{85}Rb and 27.8% ^{87}Rb) before being recorded by an avalanche photodiode (Hamamatsu C5460). The majority of the laser beam passes to the probe volume. A series of six anti-reflection coated lenses are used to collect the scattered light from the probe volume and relay it through a Rb cell identical to that in the reference arm, a ±1 nm narrow-band filter (Barr Associates) and focus it onto a side-looking PMT (Hamamatsu R636-10). The PMT is biased at ~1000 V to give good radiant sensitivity while maintaining a linear response. The narrow band filter greatly reduces interference from ambient light while passing the Rayleigh scattered signal with high efficiency (80% peak transmittance). For these preliminary experiments we chose standard off-the-shelf lenses for the scattering arm optics. The lenses were

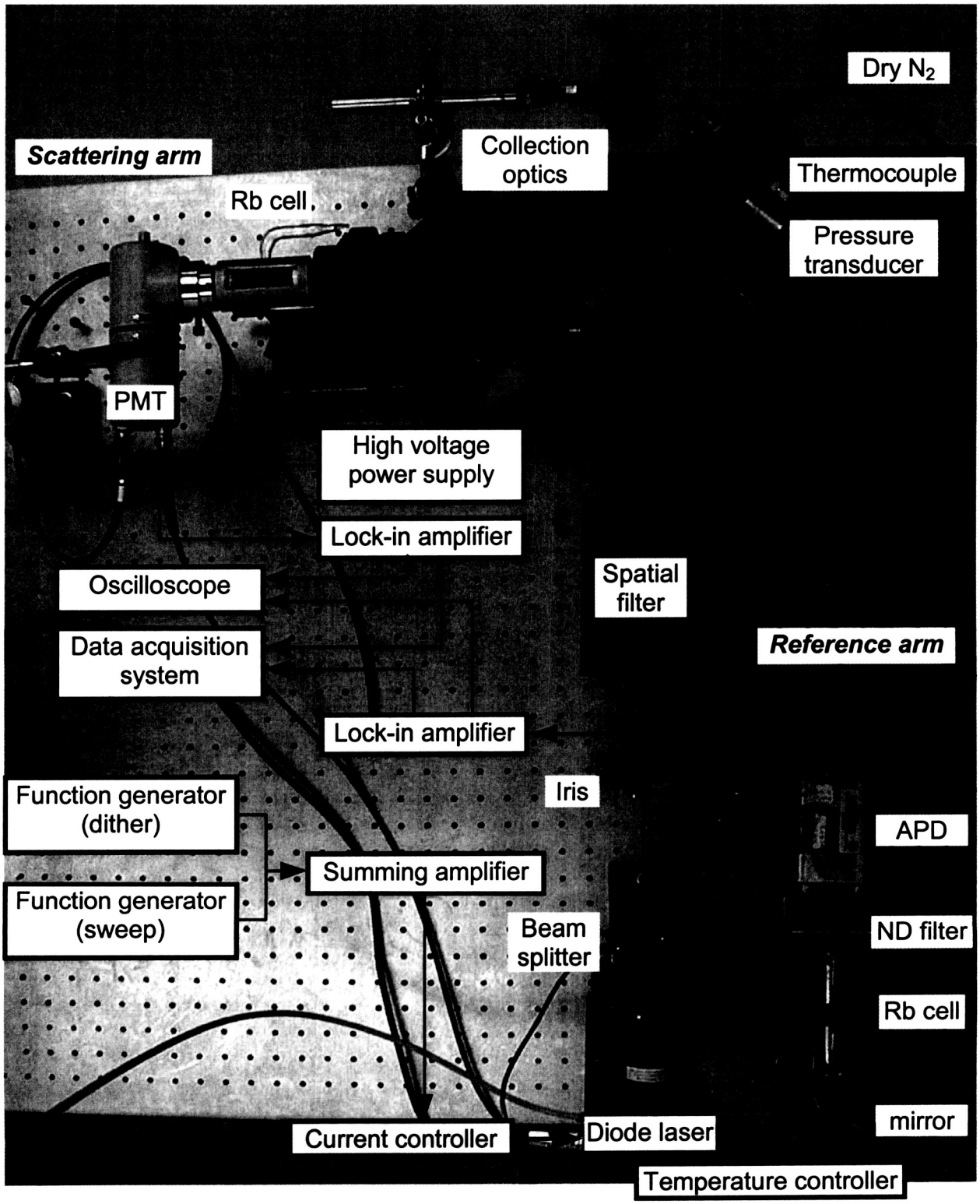

Fig. 2 MFRS experimental setup

chosen with the help of OSLO LT freeware, with a design objective of filling the PMT photocathode with high transmission efficiency. The collection F/# of ~1.2 was achieved using a pair of 100mm diameter, 120.8 mm focal length plano-convex lenses (Melles Griot LPX215/076).

Two lock-in amplifiers (Stanford Research Systems SR830) are synchronized with the modulation signal and run in *2f* mode so that their output approximates the 2nd-derivative of the Rb D_2-profile. The lock-in outputs signals are digitized with a 1.25 Msample/s, 12-bit National Instruments data acquisition board (PCI-MIO-16E-1). A virtual instrument (VI) was developed with National Instruments LabView G-programming language to trigger acquisition and save the acquired profiles to a binary file.

A converging nozzle with an exit diameter of 3.1 mm (1/8-in) is used to provide an well characterized flow. A relatively rapid acceleration is provided by a 12.5 mm (1/2-in) radius of curvature up to the throat, and isentropic expansion is assumed in the core flow. The maximum theoretical velocity of the jet, expanding isentropically to atmospheric pressure, is readily calculated from the measured stagnation pressure P_o and temperature T_o in the plenum just upstream of the nozzle:

$$V = \left[\frac{2\gamma R T_o}{\gamma - 1} \left\{ 1 - \left(\frac{P_{atm}}{P_o} \right)^{\frac{\gamma}{\gamma - 1}} \right\} \right]^{\frac{1}{2}} \tag{3}$$

where $\gamma = 1.4$ and $R = 297$ J/kg K for N_2.

The experiment is set to collect Rayleigh scattering at right angles to the laser beam, with the jet axis bisecting this angle (see Fig. 2). Equation 1 shows that in this geometry the velocimeter measures the axial velocity of the jet. A post-processing VI was written to cross-correlate the signal and reference profiles, and to convert the Doppler frequency shift to a velocity measurement. Figure 3 shows a sample screen from this VI after post-processing the measurements presented here.

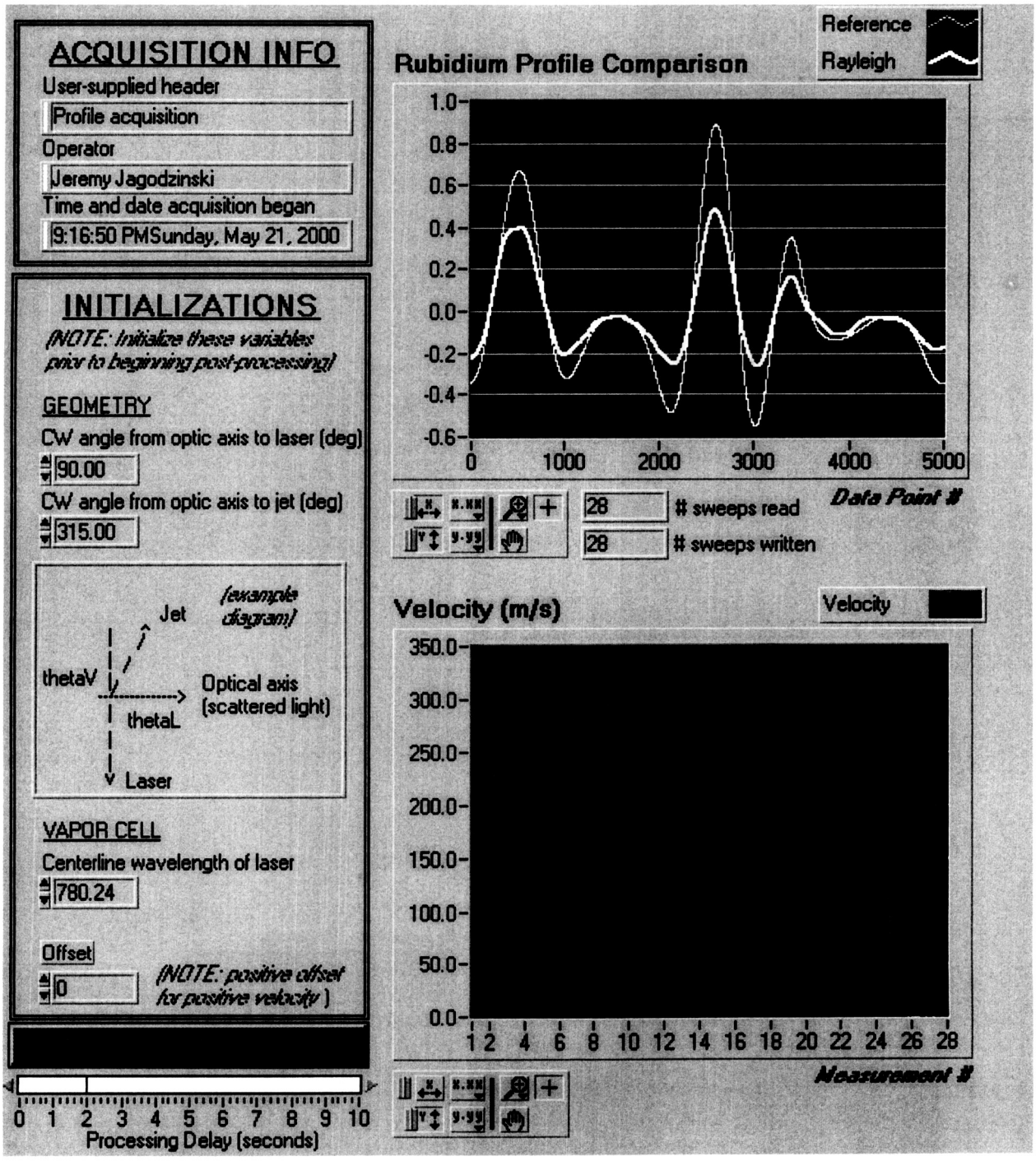

Fig. 3 LabView post-processing routine

4. SWEEP MODE EXPERIMENTS

Velocity measurements were made nominally 9 nozzle diameters (28 mm) downstream of the jet. In these preliminary experiments with molecular Rayleigh scattering the imaged length ℓ of the probe volume is estimated to be ~5 mm so the measurements average over flow gradients and cannot be directly compared to a calculated jet velocity field. The imaged region was kept large in these measurements because we were establishing the feasibility of making measurements in unseeded flows with a low power laser.

Figure 4 shows the data for the Doppler-shifted Rayleigh scattered signal and the reference signal collected during a single sweep of the laser. The sweep frequency was 0.1 Hz and the laser was swept through approximately 4 GHz to cover the two strong absorption features of ^{85}Rb that are separated by about 3 GHz. The reduced sweep range enables the profile to be scanned with lower distortion for a given sweep rate. The laser frequency was modulated at the rate of 2 kHz with a modulation amplitude of approximately 300 MHz and the lock-in output time constant was set to 100 ms.

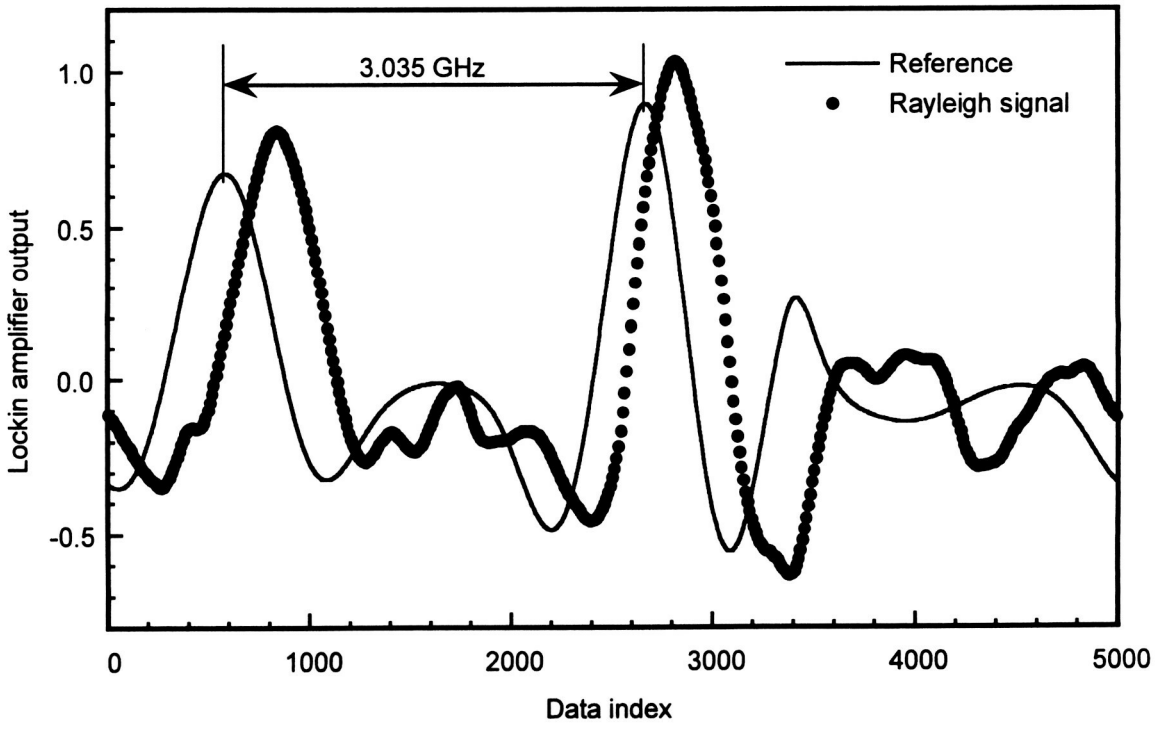

Fig. 4 Doppler-shifted Rayleigh scattered signal from supersonic jet of N_2 compared to reference signal measured in a static cell.

Figure 5 summarizes the results of a series the velocity measurements obtained during a single run. Velocities were calculated by computer processing of the acquired data using the LabView VI. The plenum pressure and temperature were recorded manually for each laser sweep (duration 10 s) and are also displayed on Fig. 5. The maximum velocity, assuming isentropic expansion from the stagnation pressure to the recorded atmospheric pressure of 98 kPa, is displayed on Fig. 5 for reference. The measured velocity tends toward the maximum theoretical velocity as the pressure in the settling chamber increases and as the temperature in the settling chamber decreases. Because of the poor spatial resolution one cannot interpret this trend in terms of changes in the flow structure. As the plenum temperature drops, the Rayleigh signal strength improves slightly, which may be attributed to an increase in number density in the probe volume.

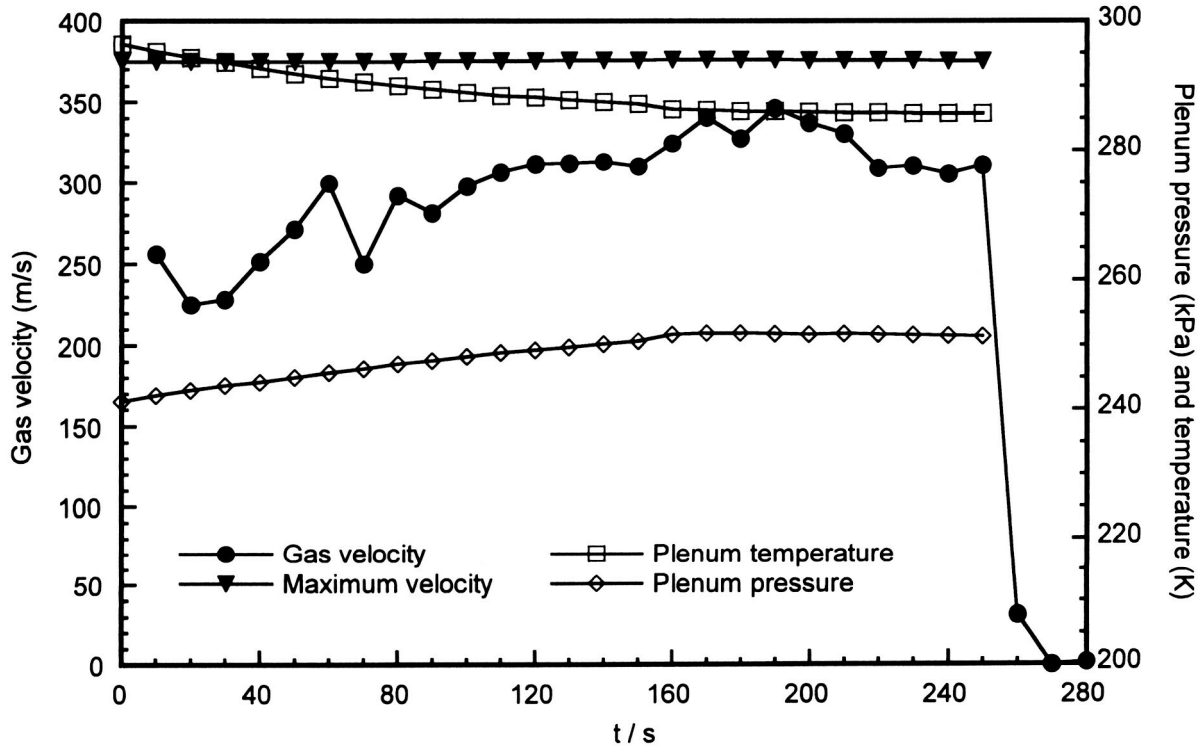

Fig. 5 MFRS velocity measurements in supersonic jet of N_2.

In these experiments we sweep through a significant portion of the hyperfine structure of Rb transition, and cross-correlate the Rayleigh scattered profile to the reference profile. A primary drawback of this mode of operation is that the temporal resolution of the velocity measurements is limited by the need to average out fluctuations in the Rayleigh scattered signal. If the mean density of the gas being interrogated is constant, then density fluctuations can be averaged-out,

provided that the time constant of the lock-in amplifier is sufficiently large. In the present experiments, with 25 mW of laser power in the probe volume, an output time constant of at least 100 ms was required to measure the Rayleigh scattered signal reliably. Ideally the ramp period should be much longer than the output time constant, and modulation period much less. With this time constant ramp frequencies greater than 0.1 Hz distorted the profile, and so the temporal resolution of the MFRS velocimeter was limited to 10 s using the present equipment. The lock-in amplifiers used in the experiment have a minimum output time constant of 10 μs and can lock to a maximum modulation frequency of 102 kHz, i.e. the minimum modulation period is 9.8 μs.

A primary drawback of this sweep mode is that the temporal resolution of velocity measurements is limited. In order to improve temporal resolution the frequency-locked mode of operation was developed.

5. FREQUENCY-LOCKED EXPERIMENTS

The diode is tuned to the edge of one of the Doppler broadened components in the multiplet and the laser is locked to the desired frequency while modulating about this frequency. A shift in the Rayleigh scattered frequency due to changes in Doppler shift results in a change in absorption and thus in the magnitude of the *2f* signal. There is additional experimental complexity in the frequency-locked mode of operation, because of the need to stabilize the laser and account for density fluctuations in the probe volume. Laser frequency drifts must be prevented because they would be misinterpreted as velocity changes. Similarly, density fluctuations in the probe volume change the scattering intensity but could be misinterpreted as velocity changes.

We use a ratioed detection scheme to provide a signal that is unaffected by density or laser power fluctuations in the probe volume. The Rayleigh scattered signal detected in the scattering arm is sent to two separate lock-in amplifiers, each set to extract a different harmonic of the modulated absorption signal. These two harmonics are then ratioed, resulting in a frequency dependent, scattering-intensity independent signal. By temperature stabilizing the Rb vapor cell in the scattering arm, a preliminary calibration sweep across the D_2 line will provide a reference ratio profile for velocity measurements in the frequency-locked mode.

Figure 6 shows the essential experimental features of the MFRS velocimeter in the frequency-locked mode of operation. A frequency tunable laser source is used to implement heterodyne detection. The beam from the laser is collimated and a small portion (<1%) of the beam is split off to a reference arm, and passes through a 10 cm long room temperature cell containing Rb vapor in natural isotopic abundance (72.2% ^{85}Rb and 27.8% ^{87}Rb) before being recorded by a silicon photodiode (Thorlabs DET110). The majority of the laser beam passes to the probe volume. A series of six anti-reflection coated lenses are used to collect the scattered light from the probe volume and relay it through a Rb cell identical to that in the reference arm, a ±1 nm narrow-band filter (Barr Associates), and ultimately to focus it onto a side-looking PMT (Hamamatsu R636-10). A high frequency modulation is imposed on the laser source, and results in a modulated absorption through the rubidium filter in the reference and scattering arm. A corresponding modulation appears in the detector outputs that are fed into lock-in amplifiers, synchronized with the function generator that drives the frequency modulation.

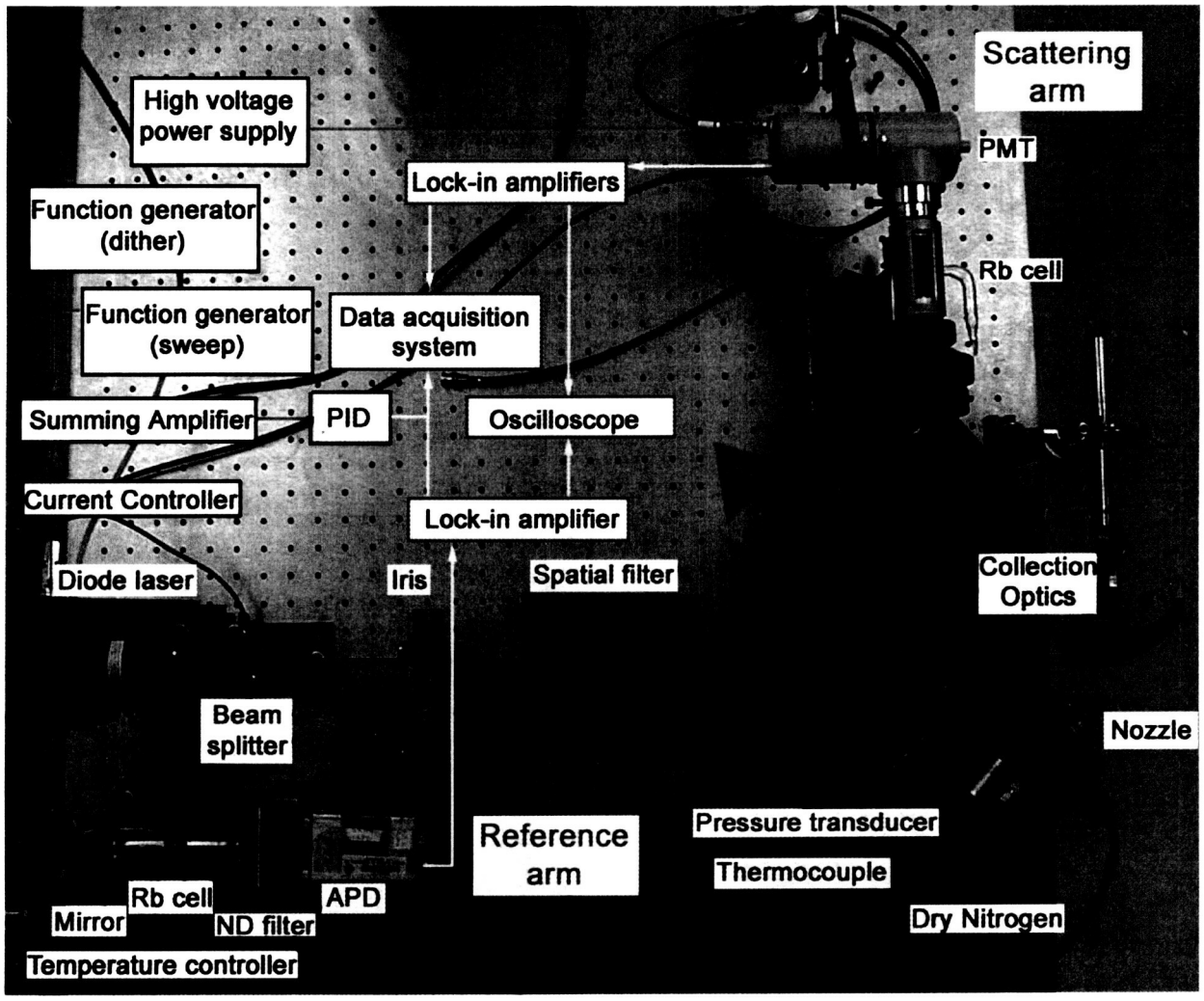

Fig. 6 Experimental Setup for the MFRS Velocimeter in the Frequency-Locked Mode of Operation

Figure 7 shows an experimental *1f/2f* ratio profile acquired by direct absorption through a Rb vapor cell. The *x*-axis velocity is calculated assuming an experimental geometry providing axial velocity measurements. The dynamic range of the ratio *mf/nf* is limited by zero-crossings of the *nf* profile which creates singularities in the ratio. However, the range is readily extended by simply inverting the ratio as shown in Fig. 7.

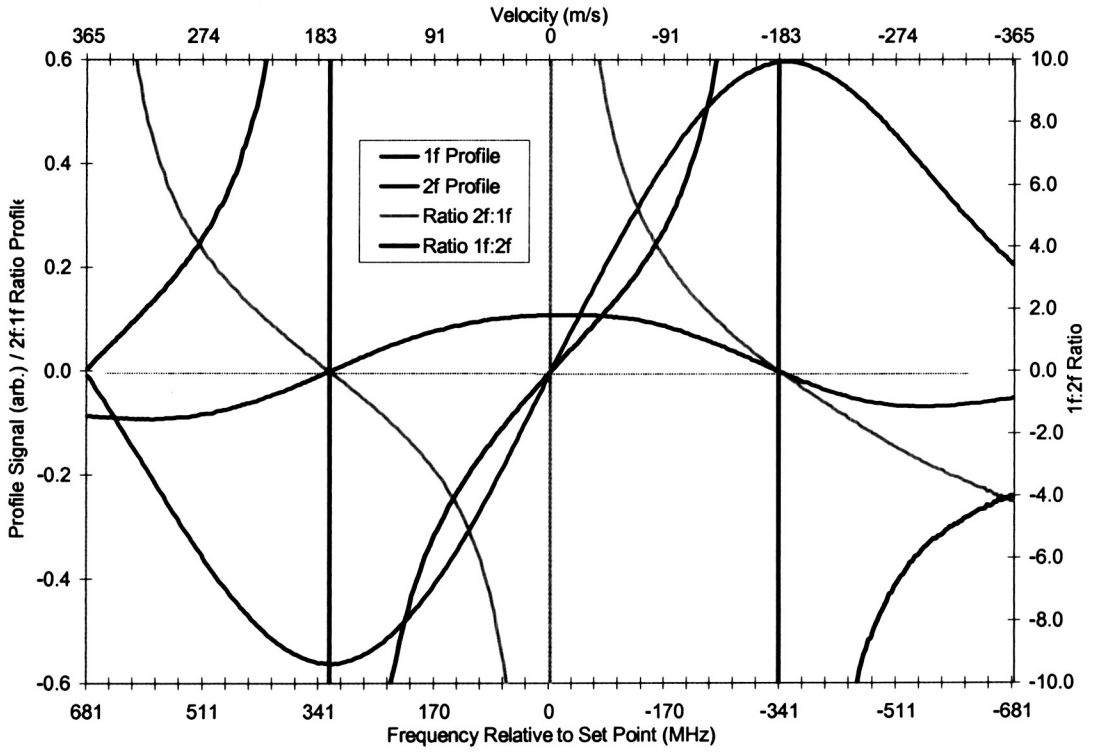

Fig. 7 Frequency Dependent, Scattering Intensity Independent Ratio Profiles

Figures 8 and 9 show some results from measurements using the ratio detection scheme. The same diode used in the sweep mode of operation (Hitachi HL7851G) was used in these experiments, providing approximately 25 mW of power to the probe volume. Prior to making velocity measurements, the experiment is operated in the sweep mode. The signal from an avalanche photodiode (APD, Hamamatsu C5460) in the reference arm was output to a lock-in amplifier (Stanford Research Systems SR530). The upper left graph in Figure 8 shows a *2f* profile acquired in the reference arm of the velocimeter while modulating the laser at 2 kHz and sweeping at 0.1 Hz.

For these preliminary investigations, the laser was stabilized in the frequency-locked mode on the positive edge of the Doppler broadened component in the *2f* profile corresponding to the F=3 level in the ground state of ^{85}Rb. The lower left graph of Fig. 8 shows velocity corresponding to the lock-in signal determined from the acquired *2f* profile. A curve fit to this line will be used in future experiments to account for minor drifts in laser frequency. The laser will be stabilized on the edge of some line of the *2f* absorption profile from the reference arm using a PID. Besides

providing the error signal for frequency stabilization, the 2nd-harmonic signal from the reference lock-in can be used to track the instantaneous frequency of the laser. Changes in the amplitude of this signal, monitored by the data acquisition system, can be used to calculate short-term drifts in laser frequency from the zero-crossing set point, and velocity measurements from the Doppler shifted Rayleigh scattered signal can be corrected accordingly.

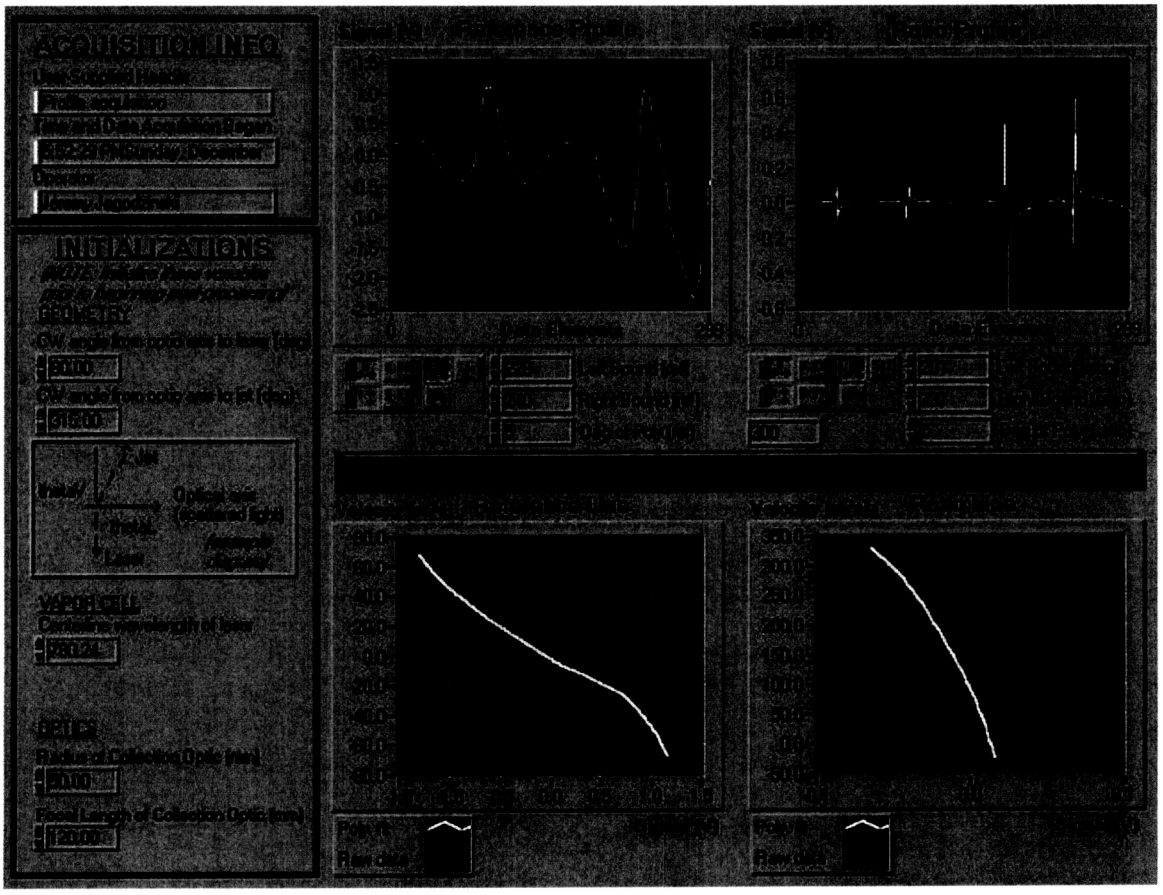

Fig. 8 Preprocessing for frequency-locked mode of operation

Rayleigh scattered light was collected from static air at STP and focused onto a PMT (Hamamatsu R636-10). The signal from the PMT was output to two lock-in amplifiers (Stanford Research Systems SR830), set to extract the 1st- and 3rd-harmonic respectively of the modulated signal. The upper right graph in Fig. 7 shows the ratio *3f/1f* of the modulated Rayleigh scattered signal from these lock-in amplifiers over the entire scan. The velocity versus signal for a portion of the ratio profile appropriate for measurement of positive velocities is shown in the lower right graph of Fig. 8. A polynomial fit to this frequency dependent, scattering-intensity independent

signal is used to determine velocity in the probe volume from the Doppler shifted Rayleigh scattered signal amplitude.

Figure 9 shows some preliminary velocity measurements taken in static air and displayed at an effective rate of 1 Hz. It should be noted that the velocity data were actually acquired at the rate of 1 kHz, but a 1000 point average taken for the screen shot displayed. The averaging did not significantly change the appearance of the data when the laser was operating properly. The large spikes in the velocity displayed are the result of mode-hops in the laser frequency. Disregarding these spikes, one sees a slight upward trend in the measured velocity, which is centered at approximately 23 m/s. The velocity offset from zero is the result of a lag in the data acquisition that will be accounted for in future work, and the upward trend results from a slow drift in the laser frequency. The diode frequency would hop off the line it was stabilized on, and it would generally take several seconds of manual adjustment to the laser current to reestablish the lock. We have since developed a MOPA system that is much more stable than the free-running diode used in these preliminary experiments.

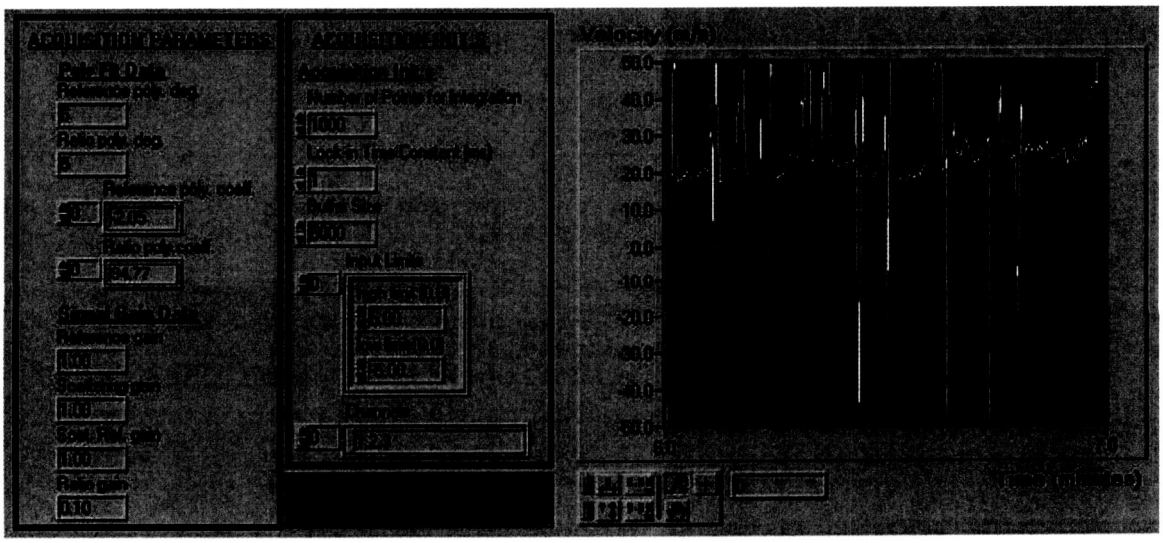

Fig. 9 Velocity measurements from static air at STP utilizing the frequency-locked mode of operation

6. PROBLEMS WITH A FREE-RUNNING DIODE LASER

A drift in laser frequency would be misinterpreted as a Doppler frequency shift of the Rayleigh scattered signal, and attributed to a change in flow velocity. Therefore, in the frequency-locked mode of operation, the reference arm is used to lock the laser to the edge of some feature in the absorption profile. The same free-running diode used in the sweep mode of operation (Hitachi HL7851G) was used in preliminary investigations into frequency stabilization. The injection current of the diode laser was dithered at a kHz rate while simultaneously sweeping the output frequency across the Rb resonance using a current ramp. The amplitude of the sweep was slowly reduced, and the dc current offset of the controller was simultaneously adjusted to tune to the frequency set point. The laser was tuned to sit on the edge of a Doppler broadened component in the *2f* profile corresponding to the F=3 level in the ground state of ^{85}Rb (Fig. 1). A proportional-integral-differential (PID) controller was built to stabilize the laser at the zero crossing of this line, providing feedback to the current controller based on the error signal due to drift in laser frequency.

We were unable to obtain satisfactory levels of frequency stability with the PID. A 60 Hz ripple, resulting from the ac-line voltage powering the current controller, is noticeable when the diode is tuned to the edge of the Doppler broadened line. The PID could not suppress this ripple adequately. When the current controller was powered from its internal batteries, the short-term frequency stability improved, but large long-term drifts in the laser frequency were observed. Naturally, the specifics of PID design must account for the dynamics of the error signal and the circuit itself. However, these specifics can be ignored when illustrating the deficiencies associated with stabilization of a free-running diode via feedback to the current controller.

If an accuracy of 1 cm/s is demanded in our velocity measurements (needed for microgravity combustion measurements), then a maximum drift in laser frequency of 18 kHz is tolerable. Laser diodes tune with injection current at a rate of approximately -2 GHz/mA. Proportional current feedback to correct for an 18 kHz drift in laser frequency is therefore O(10 nA). The transfer function for the external modulation input of the ILX Lightwave LDX-3620 current controller used in the experiment is 100 mA/V. A proportional voltage feedback from the PID to the current controller of O(100nV) is therefore necessary to correct for an 18 kHz drift in laser frequency. At these signal levels, any noise coupled into the external modulation input of the

current controller will overwhelm the feedback signal. The ultraprecision OP177EZ op amp used in the PID, for instance, has an input noise voltage of 118 nV rms and input offset voltage drift of 100 nV/°C.

7. EXTENDED CAVITY DIODE LASER SOURCE

An extended-cavity diode laser (ECDL) has been built to avoid the difficulties associated with stabilization of a free-running diode; the feedback levels for frequency stability of the ECDL are significantly larger than those used to stabilize the free-running diode. ECDLs use a wavelength selective element (e.g. etalon, prism, grating) to provide optical feedback to the laser junction.[13,17] Specifically, we have built an ECDL in the Littrow configuration,[18-22] as shown in Figure 10. The rear facet of the diode forms one end of the cavity and the diode junction provides gain. A grating at the Littrow angle to the rear facet forms the other end of the cavity, the 1st-order diffraction providing optical feedback to the diode junction and the 0th-order diffraction (reflection) exiting the cavity.

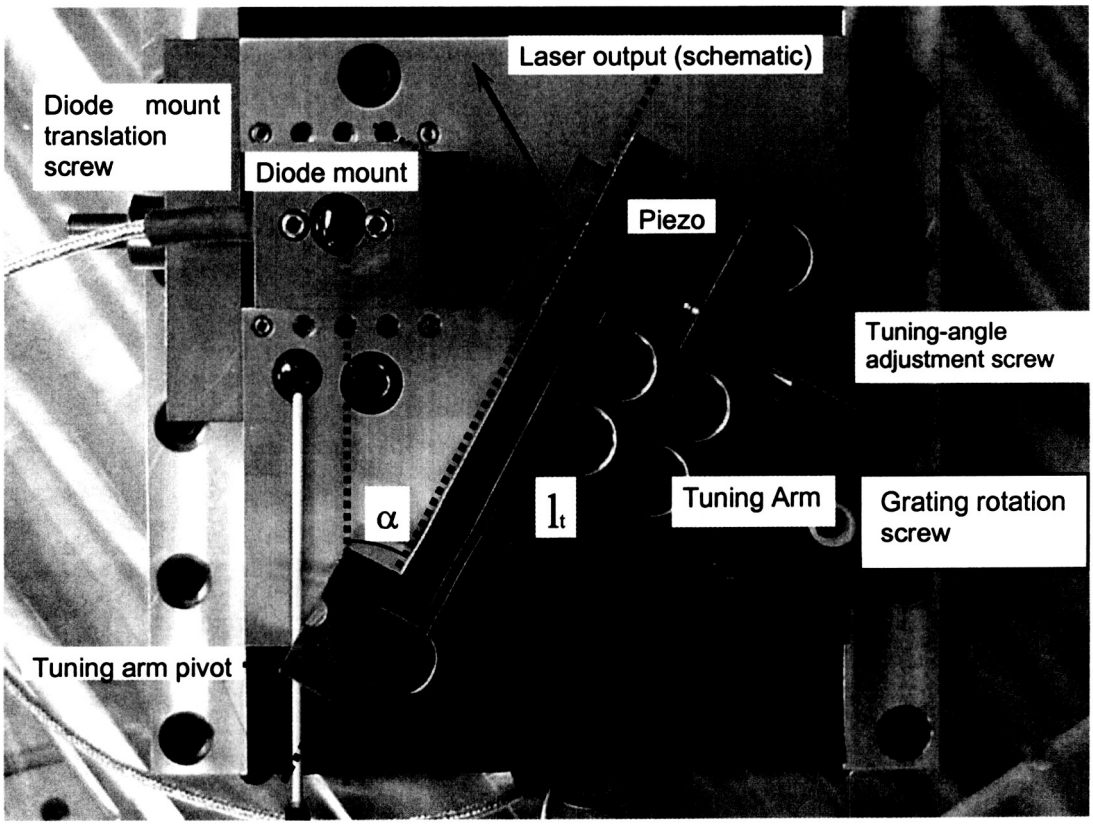

Fig. 10 Photograph of the Littrow cavity stabilized laser assembly.

The basic geometry of the Littrow laser is dictated by the grating equation,

$$d\left(\sin\alpha_o + \sin\beta_o\right) = m\lambda_o, \tag{4}$$

where d is the groove width (0.83 μm for the 1200 lines/mm grating we used in our cavity), m is the diffraction order (we operate the grating in 1st-order), λ_o is the centerline wavelength of the diffracted beam, α_o is the angle of the incident beam relative to the grating normal, and β_o is the angle of the diffracted beam at λ_o relative to the grating normal. Placing the grating at the Littrow angle we find $\alpha_o = \beta_o = 27.9°$ for operation at $\lambda_o = 780$ nm.

The cavity is tuned in frequency by changing the grating angle. For continuous wavelength tuning, the extended-cavity mode structure has to synchronously track changes in the feedback frequency. As the grating angle is changed, generating a change in the feedback frequency, the phase in the external cavity formed by the rear facet of the diode and the grating must remain unchanged for synchronous tuning. The optimal configuration for synchronous tuning can be derived using scalar diffraction theory[23] by considering the phase accrual in the external cavity. Placing the grating rotation pivot at the intersection of the rear facet of the diode and the grating plane minimizes phase changes in the cavity.[24] In addition, we minimized the external cavity length l_c with the intention of increasing the free spectral range of the cavity, thereby minimizing the sensitivity of the cavity to any phase changes that do occur and improving the chances of mode-hop free synchronous tuning. A cavity length of l_c = 31.75 mm was chosen to avoid obstruction of the output beam by the diode mount.

AR coated diodes are critical for the design of a predictable, user-friendly, tunable laser system.[25] Without AR-coating, wavelength tuning is an intricate balance between the gain profile of the active region of the diode, the diode cavity modes, and the external cavity modes. AR coating lends predictability to the ECDL, allowing the operator to essentially ignore oscillations in the diode cavity. Our Littrow cavity uses an AR coated diode (Sacher-Laser SAL-780-40) with a quoted front facet reflectivity of $R<1.9\times10^{-6}$ and a rated power of 40 mW before AR coating. The diode is mounted in a collimation tube with an f=11.0 mm, 0.25NA aspheric collimation optic (Thorlabs LT220P-B). The collimation tube is mounted in a metal block that can be translated along the optical axis of the laser beam, allowing the rear facet of the diode laser to be correctly positioned with respect to the grating pivot. An 80-pitch screw (New Focus 9301-K) provides adjustment.

Index guided diode lasers are polarized perpendicular to the fast optical axis, so to maximize the resolution of the grating we were forced to use the grating in the S-plane (i.e. with the

polarization parallel to the rulings). A relatively inexpensive, gold-coated, ruled grating (1200 lines/mm) from Edmund-Scientific (NT43-848) with a S-plane 1st-order efficiency of approximately 55% was chosen to provide sufficient levels of optical feedback to the diode junction. The grating is mounted to a tuning arm, with coarse angle tuning provided by an 80-pitch adjustment screw (New Focus 9301-K) and fine adjustment provided by a piezoelectric transducer (Thorlabs AE0505D08). The tuning arm is mounted to a baseplate. A vertical adjustment screw (New Focus 9313-K) in the baseplate allows for adjustment of the grating plane angle relative to the tuning arm axis. On a recommendation from Windell Oskay and Daniel Steck, then with the Atom Optics Group at The University of Texas at Austin, we used flexure joints for the tuning arm and baseplate pivots[18-19] and machined the cavity from 954 Aluminum-Bronze, a relatively elastic alloy with a high thermal mass.

A low-noise current controller (ILX Lightwave LDX-3620) provides power to the AR coated diode in the cavity, and a spectroscopic grade thermoelectric temperature controller (ILX Lightwave LDT-5910B) provides temperature control to a 30 W thermoelectric cooler (Marlow Industries ST3353) mounted to the baseplate of the cavity. Temperature control is based on a 10 K NTC thermistor (Omega 44006). An amplified sweep voltage and modulation voltage are applied to the piezo attached to the tuning arm to sweep and dither the frequency of the Littrow laser. A function generator provides a sawtooth sweep voltage and one of the lock-in amplifiers provides a sine wave modulation voltage, both of which are amplified by a regulated high-voltage amplifier of our own design. The laser is frequency stabilized by slowly reducing the sweep amplitude while simultaneously adjusting the offset voltage of the high voltage amplifier, as shown in Figure 4. With the sweep completely turned off, the PID is turned on to provide feedback based on an error signal in the reference arm of the experiment. For our preliminary investigations we decided to tune the laser to the zero crossing of a Doppler broadened component in the *1f* profile corresponding to the F=3 level in the ground state of ^{85}Rb, as shown in Figure 4. The frequency at each zero-crossing of the *1f* profile is independent of the temperature in the Rb vapor cell, and though temperature fluctuations in the cell change the slope of the error signal to the PID, the resulting changes in stabilization feedback gain to the Littrow cavity can be ignored for ambient temperature fluctuations.

Operating the grating in 1st-order at the Littrow angle, Eq. 4 can be recast as

$$\sin\alpha_o = \frac{\lambda_o}{2d}, \tag{5}$$

from which the tuning performance of the Littrow laser is easily derivable,

$$\frac{\Delta\lambda}{\Delta\alpha} = -\lambda_o \cot\alpha_o . \tag{6}$$

For fine angle tuning provided by the piezoelectric transducer attached to the tuning arm of the cavity,

$$\Delta\alpha \cong \frac{D_V V}{l_t}, \tag{7}$$

where D_V is the axial displacement of the piezo stack per unit voltage (approximately 61 nm/V), V is the voltage applied to the piezo stack, and l_t is the length from the grating pivot to the optical axis of the diode beam along the grating plane (67.8 mm), as shown in Figure 10. Combining Eqs. (6) and (7), and noting that

$$\Delta\nu = -\frac{c}{\lambda_o^2}\Delta\lambda, \tag{8}$$

we find that the Littrow cavity tunes in frequency with applied voltage to the piezo according to the following equation:

$$\left.\frac{\Delta\nu}{V}\right|_{EDCL} \cong \frac{D_V}{l_t}\nu_o \cot\alpha_o . \tag{9}$$

Operating at a centerline frequency of ν_o = 3.85×1014 Hz with the corresponding Littrow angle of α_o = 27.9°, we calculate a tuning performance for our Littrow cavity of $\Delta\nu/V|\,\mathrm{ECDL} \cong 0.6$ GHz/V. Reconsidering our previous example, if an accuracy of 1 cm/s is demanded in our velocity measurements then a maximum drift in laser frequency of $\Delta\nu_{error}$ = 18 kHz is tolerable. In this case, the level of proportional feedback to the tuning arm of the Littrow cavity is,

$$\Delta V_{feedback} = \mathrm{O}\left(\frac{\Delta\nu_{error}}{\left.\frac{\Delta\nu}{\Delta V}\right|_{ECDL}}\right) = \mathrm{O}(30\mu\mathrm{V}) . \tag{10}$$

These feedback levels are about two orders of magnitude higher than the O(0.1 μV) levels required to stabilize the free-running diode laser to the same precision and well above noise levels. This is the primary reason for building the Littrow cavity.

Laser power in the probe volume remains a concern since the laser system is to be used for Rayleigh scattering experiments. Relatively high power (~100 mW) single-mode diode lasers at 780 nm are commercially available. However, we have had limited success using several such diodes in a stand-alone configuration. We considered using them in the ECDL we built, but these higher power diodes are not generally available with AR coating for a reasonable price. Without AR coating, the required feedback from the grating would greatly reduce the power coupled out of the external cavity. The advantage in power these diodes have over lower cost, lower power, AR coated diodes is negligible when they are configured in a grating feedback ECDL. For instance, the maximum power obtained from an ECDL using a commercially available 100 mW diode laser without AR coating (STC model LT50 from Spectra Diode Labs) while maintaining good spectral control was 15 mW.[17] We have measured an output power of 10 mW from our Littrow cavity using a 40 mW AR-coated diode.

To obtain higher power with good spectral quality we have been developing an injection-locked laser system, whereby a single-mode master oscillator injects a broad area laser (BAL) diode. Stand-alone BAL diodes exhibit poor temporal and spatial coherence, but can be configured to track the spectral performance of the master oscillator with good spatial quality. Commercially available broad stripe diodes, with no AR coating on the front facet, operate under injection as saturable multi-pass amplifiers.[26] To obtain a single spatial mode, the master oscillator injects in only a few spatial modes of the slave laser. With enough injection power, the injected modes are favored over the non-injected modes (i.e. the injected modes saturate the slave).[17] Under the appropriate conditions, the locked broad stripe diode tracks the longitudinal mode of the master oscillator with good spatial quality. The maximum attainable power from the slave is determined by the master injection power and the coupling efficiency of the injected beam. Pawletko, *et al.* demonstrated 120 mW of output power at 794 nm in a single diffraction-limited Gaussian spot by injecting a 500 mW broad stripe (Coherent S-81-500C-100-Q) with 2.6 mW of power from a grating feedback master oscillator.[26] Iida *et al.* obtained 550 mW from a commercially available 1 W broad stripe diode (Sony SLD304XT) with 25 mW of injection power.[27] The injection-locking system we developed utilizes an AR coated 1.5 W broad stripe diode with a stripe length of 100 μm (Sacher-Laser BA-780-100). In essence, we are building a master oscillator power amplifier (MOPA) system, with the AR coated broad stripe diode serving as a power amplifier of the single-mode output from our Littrow cavity.

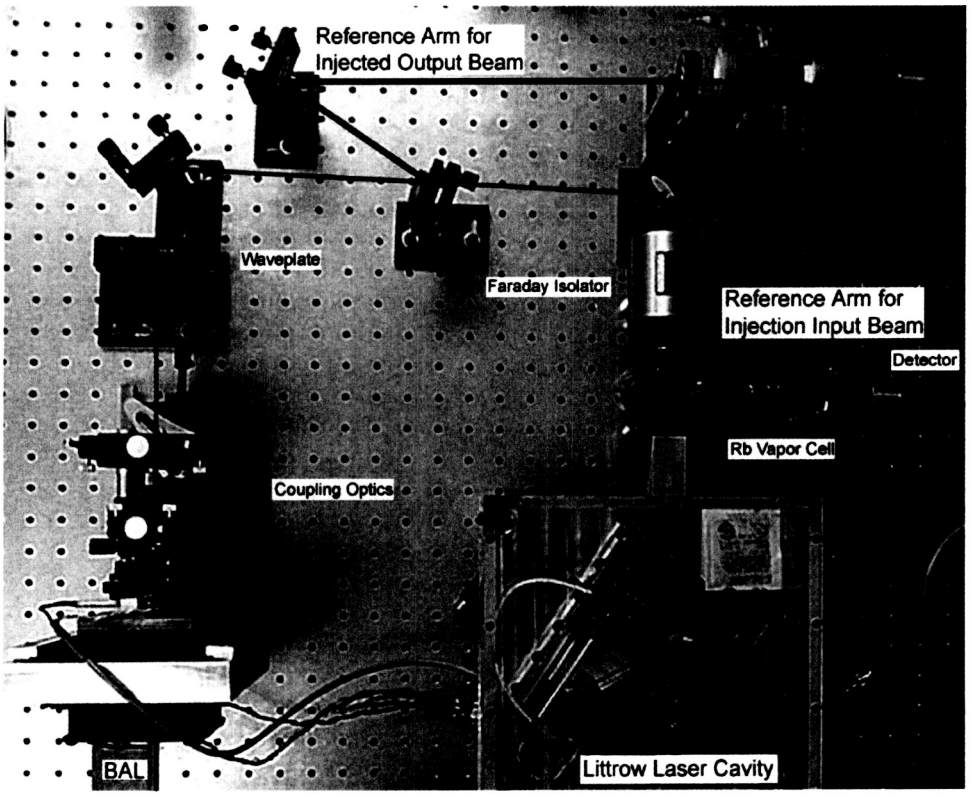

Fig. 11 Injection-Locked Laser System

Figure 11 is a picture of the injection-locked laser system. A small portion (<1%) of the Littrow output is split off to a reference arm, and passes through a Rb vapor cell before being recorded by a Si photodiode (Thorlabs DET110); The reference arm enables us to tune the Littrow cavity to the D_2-line of Rb. In our experience, an isolator at the exit of the Littrow laser is necessary to prevent the BAL output from being coupled into the cavity. A Faraday isolator (Optics for Research IO-5C-780-VLP-Z) provides 42 dB of isolation between the Littrow laser and the BAL. After passing through the isolator, the Littrow laser beam is guided through a $\lambda/2$-wave plate and a series of three coupling optics, which focus the collimated injection beam into the BAL junction. The BAL is mounted to a Cu cold plate, which is mounted to a 30 W thermoelectric cooler (TEC) (Marlow Industries ST3353). A spectroscopic grade temperature controller (ILX Lightwave LDT-5910B) provides temperature control to the TEC based on a signal from a 10 K NTC thermistor (Omega 44006). A 500 mA low-noise current controller

(ILX Lightwave LDX-3620) was used in our preliminary experiments to provide power to the BAL.

The spatial beam profiles of the Littrow laser and the BAL must be carefully matched in order to couple the injection beam into the BAL junction. This is most easily accomplished, considering the coupling optics involved, by preserving the junction orientation between the Littrow laser and the BAL (i.e. the fast axis optical axis of the BAL is aligned with the fast optical axis of the Littrow laser). Index guided diodes are polarized parallel to their junction, however, whereas broad stripe diodes are polarized perpendicular to their junction. The $\lambda/2$-wave plate is therefore required to match the polarizations of the Littrow laser and the BAL. We have found that the coupling optics are critical to achieving amplification. By the end of the grant period we had shown that the BAL gave narrow band output that tracked the injection but had not yet achieved amplification. Amplification has since been achieved but the system is not yet optimized.

8. PRELIMINARY RESULTS WITH THE ECDL

For our preliminary attempts to frequency stabilize the Littrow cavity we tuned the laser to the zero crossing of a Doppler broadened component in the *1f* profile corresponding to the F=3 level in the ground state of ^{85}Rb. Figure 12 shows the *1f* signal of the modulated Littrow laser output with the sweep turned off. The modulation frequency was 2.09 kHz and the lock-in time constant was 3 ms. The dashed line shows the *1f* signal with the PID turned off and the solid line shows the signal with the PID providing proportional feedback to the piezo stack attached to the tuning arm. With the PID turned on, the Littrow laser exhibits frequency stability < 1MHz based on the error signal of the *1f* signal in Figure 12. The differentiator and integrator in the PID were not employed in our preliminary attempts to frequency stabilize the Littrow laser; incorporating the differentiator should improve the short-term stability, while introducing integration into the feedback signal should improve the long-term stability.

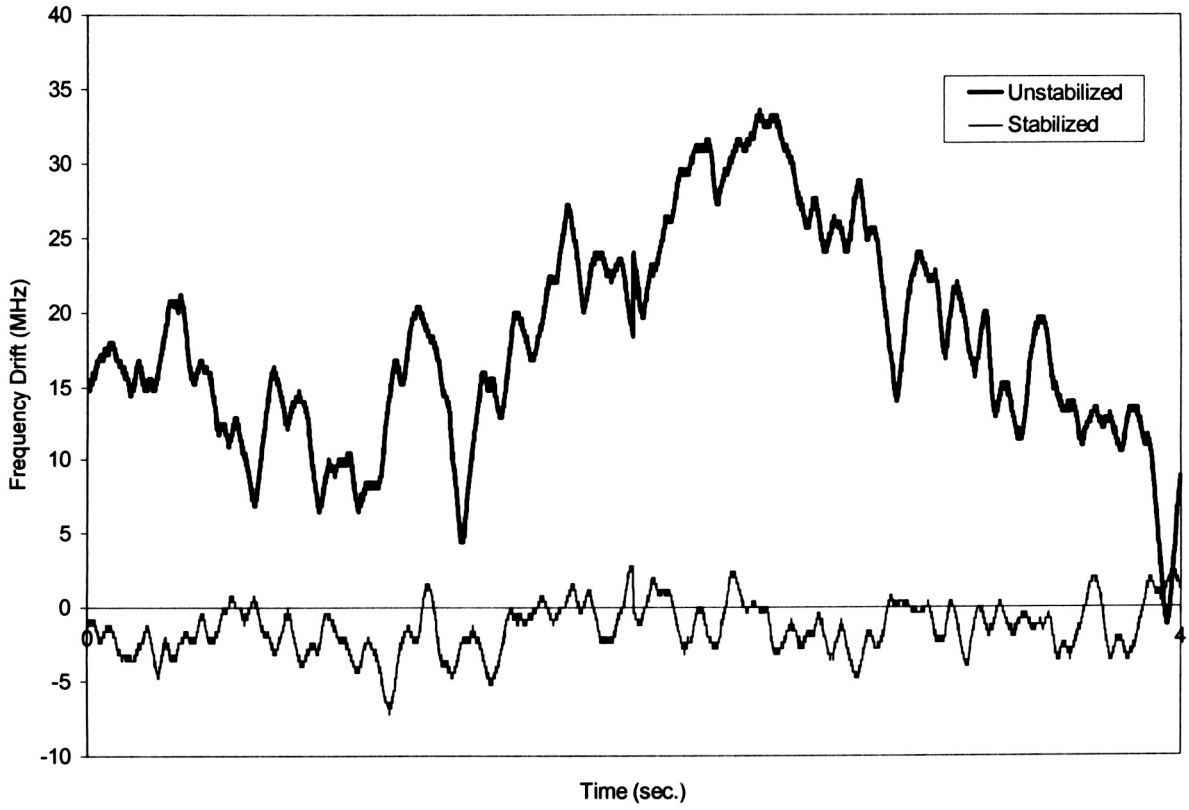

Fig. 12 Comparison of the *1f* Signal from the Stabilized and Unstabilized Littrow Cavity

As noted above, we were not able to demonstrate power amplification with our injection-locked laser system by the end of the grant period. An injection power of 2.9 mW entered the coupling optics, but only 1.2 mW of injected output power was measured. However, we have demonstrated successful slaving of the BAL laser to the master oscillator.

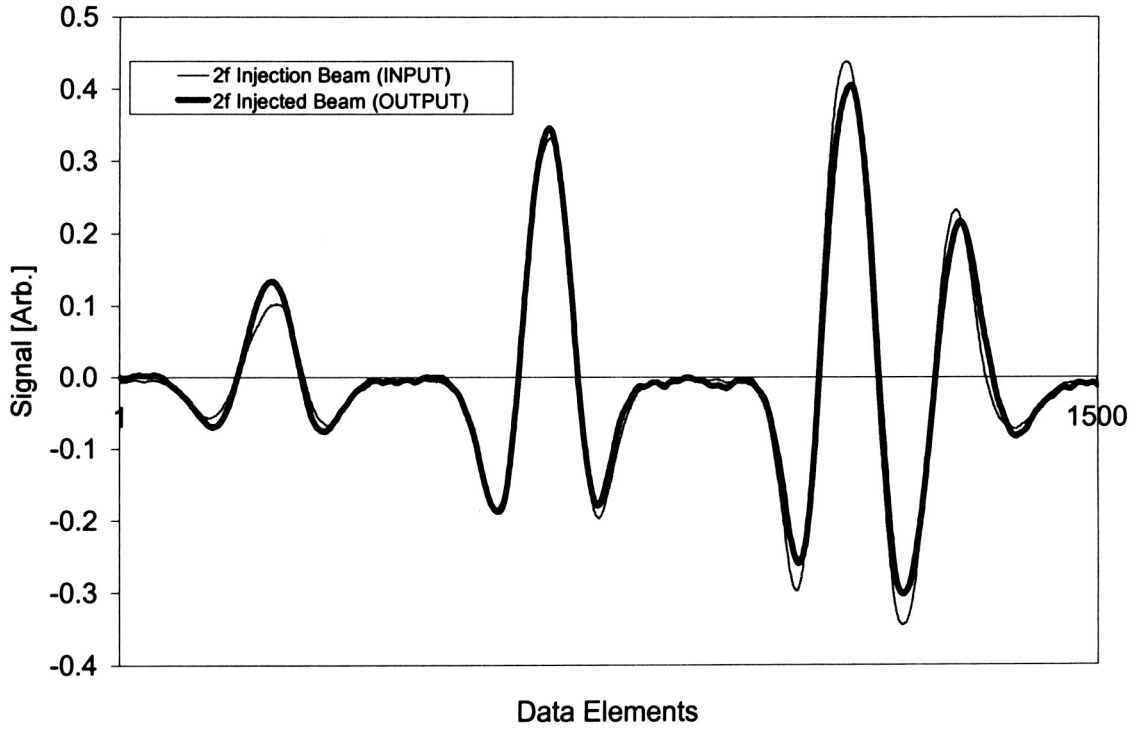

Fig. 13 *2f* Profiles of the Injection Input Beam and the Injected Output Beam

Figure 13 shows a *2f* profile of the injection input beam from the Littrow laser cavity and a *2f* profile of the injected output beam from the BAL. The modulation frequency was 2.09 kHz, the sweep frequency was 0.5 Hz, and the time constant of both lock-in amplifiers was 3 ms. The BAL was operated at a constant injection current of 497 mA; sweep and modulation of the injected output frequency were imposed by the sweep and modulation of the Littrow laser frequency. The figure clearly demonstrates that the injected output is tracking the spectral performance of the Littrow laser. The BAL that we are using has a quoted spectral width of 2 nm, or approximately 1 GHz according to Eq. (7). This is nearly twice the spectral width of the Doppler broadened multiplets in the D_2-line of Rb; the multi-mode spectral output from the BAL could not resolve the absorption features of the D_2-line. Differences between the profiles are likely the result of power fluctuations in the injected output, which our ratio detection scheme

would compensate for. The spectral performance of BAL injection has been investigated in several labs by measuring the beat note between the injection input and the injected output.[40-43] In all cases, the width of the resulting beat note is determined by the resolution of the spectrum analyzer employed (ranging from 1.5 kHz to 30 kHz).

9. CONCLUSIONS

We had developed Modulated Filtered Rayleigh Scattering for velocity measurements in unseeded gas flows. We developed the frequency-locked mode of operation with in-situ intensity referencing to make velocity measurements at high temporal rates. We developed an all-solid-state extended cavity diode laser pumping a broad area diode laser to provide a spectroscopic grade compact tunable source that could be used as the laser source. By the end of the grant period we had demonstrated that the slave laser was locked to the injection laser but had not been able to demonstrate amplification. Subsequent to the expiration of the grant we were able to demonstrate amplification of a factor of three and are optimistic that amplification by at least another order of magnitude is achievable with the current set-up.

10. REFERENCES

1. J. J. Mach and P. L. Varghese, "Velocity Measurements by Modulated Filtered Rayleigh Scattering Using Diode Lasers," *AIAA J.* **37(6)**, pp. 695-699, (1999).
2. R. Miles and W. Lempert, "Two-dimensional measurement of density, velocity, and temperature in turbulent high-speed air flows by UV Rayleigh scattering," *Applied Physics B* **51**, pp. 1-7 (1990).
3. J. A. Lock, R. G. Seasholtz, and W. T. John, "Rayleigh-Brillouin scattering to determine one-dimensional temperature and number density profiles in a gas flow field," *Applied Optics* **31**, pp. 2839-2848 (1992).
4. D. Hoffman, K. –U. Munch, and A Leipertz, "Two-dimensional temperature determination in sooting flames by filtered Rayleigh scattering," *Optics Letters* **21**, pp. 525-527 (1996).
5. J. S. Friedman, C. A. Tepley, P. A. Castleberd, and H. Roe, "Middle-atmospheric Doppler LIDAR using an iodine-vapor edge filter," *Optics Letters* **22**, p. 1648 (1997).
6. H. Shimizu, S. A. Lee, and C. Y. She, "High spectral resolution LIDAR system with atomic blocking filters for measuring atmospheric parameters," *Applied Optics* **22**, pp. 1373-1381 (1983).
7. J. A. Shirley and M. A. Winter, "Air-mass flux measurement system using Doppler-shifted filtered Rayleigh scattering," AIAA Paper 93-0513, AIAA 31st Aerospace Sciences Meeting, Reno, NV (1993).
8. G. S. Elliot and M. Samimy, "A molecular filter based technique for simultaneous measurements of velocity and thermodynamic properties," AIAA Paper 96-0304, AIAA 34th Aerospace Sciences Meeting, Renom NV (1997).
9. R. L. McKenzie, "Planar Doppler velocimetry performance in low-speed flows," AIAA Paper 97-0498, AIAA 35th Aerospace Sciences Meeting, Reno, NV (1997).
10. J. J. Mach, "Diode laser velocimetry using modulated filtered Rayleigh scattering," MS Thesis, The University of Texas at Austin, 1998.
11. J. T. Salmon and M. Laurendeau, "Calibration of laser-saturated fluorescence measurements using Rayleigh scattering," *Applied Optics* **24(1)**, pp. 65-73 (1985).
12. R. Penndorf, "Tables of the refractive index for air and the Rayleigh scattering coefficient for the spectral region between 0.2 and 20.0μ and their application to atmospheric optics," *J. Opt. Soc. Am.* **47**, p. 176 (1957).
13. C. E. Weiman and L. Hollberg, "Using diode lasers for atomic physics", *Rev. Sci. Inst.* **62(1)**, pp. 1-20, (1991).
14. Stanford Research Systems, "Application note #3: About lock-in amplifiers," Scientific and Engineering Instruments Catalog (1998-1999).
15. J. A. Silver, "Frequency modulation spectroscopy for trace species detection: theory and comparison among experimental methods," *Applied Optics* **31**, p. 707 (1992).
16. J. Reid and D. Labrie, "Second-harmonic detection with tunable diode lasers – Comparison of experiment and theory," *Applied Physics B* **26**, pp. 203-210 (1981).
17. Labachelerie, M., Latrasse, C., Kemssu, P., and Cerez, P., "The frequency control of diode lasers", *J. Phys. III France* **2**, pp. 1557-1589 (1992).
18. K. B. MacAdam, A. Steinbach, and C. Wieman, "A narrow-band tunable diode laser system with grating feedback, and a saturated absorption spectrometer for Cs and Rb," *Am. J. Phys.* **60** (12), pp. 1098-1111 (1992).

19. L. Ricci, M. Weidemüller, T. Esslinger, A. Hemmerich, C. Zimmermann, V. Vuletic, W. König, and T. W. Hänsch, "A compact grating-stabilized diode laser system for atomic physics," *Optics Comm.* **117**, pp. 541-549 (1995).
20. T. Kiguchi, A. Uematsu, M. Kitano, and H. Ogura, "Grating External Cavity Diode Lasers with Broad Tunable Range and Narrow Spectral Linewidth for High-Resolution Spectroscopy," *Jpn. J. Appl. Phys.* **35**, pp. 5890-5895 (1996).
21. C. Wieman, G. Flowers, and S. Gilbert, "Inexpensive laser cooling and trapping experiment for undergraduate laboratories," *Am. J. Phys.* **63** (4), pp. 317-330 (1995).
22. W. R. Trutna, Jr. and P. Zorabedian, "Research on External-Cavity Lasers," Hewlett-Packard Journal, pp. 35-38 (1993).
23. Born, M. and Wolf, E., Principles of Optics, 7th (Expanded) Edition, Cambridge University Press, pp. 412-443 (1999).
24. P. McNicholl and H. J. Metcalf, "Synchronous cavity mode and feedback wavelength scanning dye laser oscillators with gratings," *Applied Opitcs* **24**, pp. 2757-2761 (1985).
25. J. Jagodzinski and P. L. Varghese, "Velocity measurements by modulated filtered Rayleigh scattering using diode lasers," AIAA Paper 2001-0848, 39th Aerospace Sciences Meeting, Reno, NV (2001).
26. T. Pawletko, M. Houssin, M. Knoop, M. Vedel, and F. Vedel, "High power broad-area diode laser at 794 nm injected by an external cavity laser," *Optics Comm.* **174**, pp. 223-229 (2000).
27. K. Iida, H. Horiuchi, O. Matoba, T. Omatsu, T. Shimura, and K. Kuroda, "Injection locking a broad-area diode laser through a double phase-conjugate mirror," *Optics Comm.* **146**, pp. 7-10 (1998).

11. PUBLICATIONS ACKNOWLEDGING THIS GRANT

1. Varghese, P. L., Mach, J. J., and Jagodzinski, J. J., "Diode Laser Velocity Measurements by Modulated Filtered Rayleigh Scattering," Fifth International Microgravity Combustion Workshop, Cleveland, May 1999, (NASA/CP-1999-208917, pp. 393-396).
2. Jagodzinski, J., and Varghese, P. L., "Diode Laser Velocity Measurements in Unseeded Flows Using Modulated Filtered Rayleigh Scattering," Paper 2000-2297, AIAA 21st Aerodynamic Measurement Technology/Ground Testing Conference, Denver, June 2000.
3. Jagodzinski, J., and Varghese, P. L., "Velocity Measurements by Modulated Filtered Rayleigh Scattering Using Diode Lasers," Paper 2001-0848, AIAA 39th Aerospace Sciences Meeting, Reno, January 2001.
4. Varghese, P. L., and Jagodzinski, J. J., "Laser Velocimeter for Studies of Microgravity Combustion Flowfields," Sixth International Microgravity Combustion Workshop, Cleveland, May 2001, (NASA/CP-2001-210826, pp. 41-44).
5. Jagodzinski, J., and Varghese, P. L., "A Diode Laser Based Velocimeter for Measurements in Unseeded Flows and Flames," Paper 2003-0405, AIAA 41st Aerospace Sciences Meeting, Reno, January 2003.

REPORT DOCUMENTATION PAGE

Form Approved
OMB No. 0704-0188

1. REPORT DATE *(DD-MM-YYYY)*	2. REPORT TYPE	3. DATES COVERED *(From - To)*
30-08-2003	Summary of Research	01/14/1999-01/14/2003

4. TITLE AND SUBTITLE

Laser Velocimeter for Microgravity Combustion Studies

5a. CONTRACT NUMBER

5b. GRANT NUMBER

NAG3-2240

5c. PROGRAM ELEMENT NUMBER

6. AUTHOR(S)

Philip L. Varghese

5d. PROJECT NUMBER

5e. TASK NUMBER

5f. WORK UNIT NUMBER

7. PERFORMING ORGANIZATION NAME(S) AND ADDRESS(ES)

The University of Texas at Austin
Dept. of Aerospace Engineering & Engineering Mechanics
1 University Station, C0600
Austin, TX 78712-0235

8. PERFORMING ORGANIZATION REPORT NUMBER

9. SPONSORING/MONITORING AGENCY NAME(S) AND ADDRESS(ES)

NASA Glenn Research Center
Space Systems and Grants Branch, MS 500-319
21000 Brookpark Road
Cleveland, OH 44135-3191

10. SPONSORING/MONITOR'S ACRONYM(S)

NASA-GRC

11. SPONSORING/MONITORING REPORT NUMBER

12. DISTRIBUTION/AVAILABILITY STATEMENT

Unlimited

13. SUPPLEMENTARY NOTES

14. ABSTRACT

A velocimeter was developed based on modulated filtered Rayleigh scattering (MFRS). The MFRS velocimeter was successfully demonstrated by making one-component velocity measurements in a supersonic expansion using molecular Rayleigh scattering in a jet of N2. These measurements were made in a sweep mode where the Rayleigh scattered profile is cross-correlated with absorption in a static cell to determine velocity. To improve temporal resolution the frequency-locked mode of operation was developed, with an in-situ referencing scheme to compensate for signal fluctuations arising from density variations in the probe volume. Spectroscopic grade (i.e. continuously tunable, single-mode) laser sources with high power (>100 mW) are not commercially available at the wavelength of interest (780 nm). We developed an all-solid-state system with a low power (~10 mW) spectroscopic grade laser source in a Littrow cavity is amplified by a broad-area diode laser. We have demonstrated that the slaved output tracks the injected input but have not yet demonstrated power gain by the end of the grant period.

15. SUBJECT TERMS

Laser diagnostics, velocity measurement, unseeded gas flow, Rayleigh scattering, diode laser

16. SECURITY CLASSIFICATION OF:			17. LIMITATION OF ABSTRACT	18. NUMBER OF PAGES	19b. NAME OF RESPONSIBLE PERSON
a. REPORT	b. ABSTRACT	c. THIS PAGE			Philip L. Varghese
U	U	U	SAR	33	19b. TELEPHONE NUMBER *(Include area code)* (512) 471-3110